Draft version July 31, 2017
Typeset using LaTeX **twocolumn** style in AASTeX61

A TROJAN HORSE APPROACH TO THE PRODUCTION OF ^{18}F IN NOVAE

M. La Cognata,[1] R.G. Pizzone,[1] J. José,[2,3] M. Hernanz,[3,4] S. Cherubini,[1,5] M. Gulino,[1,6] G.G. Rapisarda,[1,5] and C. Spitaleri[1,5]

[1] *INFN - Laboratori Nazionali del Sud, Catania, Italy*
[2] *Departament de Física, EEBE, Universitat Politècnica de Catalunya, 08019 Barcelona, Spain*
[3] *Institut d'Estudis Espacials de Catalunya, E-08034 Barcelona, Spain*
[4] *Institut de Ciencies de l'Espai (ICE-CSIC). Campus UAB. c/ Can Magrans s/n, 08193 Bellaterra, Spain*
[5] *Dipartimento di Fisica e Astronomia, Università degli Studi di Catania, Catania, Italy*
[6] *Facoltà di Ingegneria ed Architettura, Kore University, Viale delle Olimpiadi, 1, 94100 Enna, Italy*

(Received ...; Revised ...; Accepted ...)

Submitted to ApJ

ABSTRACT

Crucial information on nova nucleosynthesis can be potentially inferred from γ-ray signals powered by ^{18}F decay. Therefore, the reaction network producing and destroying this radioactive isotope has been extensively studied in the last years. Among those reactions, the ^{18}F(p,α)^{15}O cross section has been measured by means of several dedicated experiments, both using direct and indirect methods. The presence of interfering resonances in the energy region of astrophysical interest has been reported by many authors including the recent applications of the Trojan Horse Method. In this work, we evaluate what changes are introduced by the Trojan Horse data in the ^{18}F(p,α)^{15}O astrophysical factor recommended in a recent R-matrix analysis, accounting for existing direct and indirect measurements. Then the updated reaction rate is calculated and parameterised and implications of the new results on nova nucleosynthesis are thoroughly discussed.

Keywords: nuclear astrophysics, novae nucleosynthesis, indirect methods, radioactive ion beams

Corresponding author: M. La Cognata
lacognata@lns.infn.it

1. INTRODUCTION

Classical novae are thermonuclear explosions occurring in the envelopes of accreting white dwarfs in stellar binary systems. The material transferred by the companion accumulates on top of the white dwarf under degenerate conditions, driving a thermonuclear runaway. The energy unleashed by the set of nuclear processes acting in correspondence of the envelope heats the material up to peak temperatures of $\sim (1-4)\times 10^8$ K. During these events, about $10^{-3}-10^{-7}$ $M_\odot$, enriched in CNO and, sometimes, other intermediate–mass elements (e.g., Ne, Na, Mg, Al) are ejected into the interstellar medium (see Starrfield, Iliadis & Hix (2008, 2016); José & Shore (2008); José (2016) for recent reviews). While classical novae have been observed in all wavelengths, spanning from radio-waves to high-energy γ-rays (with $E > 100$ MeV), they have been quite elusive in the $\sim 0.1-1$ MeV range, where emission from few radioactive nuclei is predicted.

The role of classical nova outbursts as potential sources of γ radiation was first reviewed by Clayton & Hoyle (1974); Clayton (1981). Two types of emission are expected. The early (or prompt) γ-ray emission (511 keV line plus continuum) is driven by the disintegration of the short-lived, β-unstable isotopes ^{13}N and ^{18}F. The decay of other medium-lived radioactive species, such as ^{7}Be and ^{22}Na, into excited states of their daughter nuclei and the following de-excitation by emission of a γ-ray photon of definite energy (478 keV for ^{7}Be, 1275 keV for ^{22}Na) generates a late γ-ray emission. Classical novae are also predicted to be partly responsible for the overall Galactic 1809 keV ^{26}Al line (see Hernanz (2008, 2014) for recent reviews).

At the physical conditions that characterise nova envelopes, the positrons emitted in the β^+-decays of ^{13}N and ^{18}F should thermalise before they annihilate with the surrounding electrons (Leising & Clayton 1987). Only ∼10% of the released positrons directly annihilate, while vast majority ∼90% is expected to form *positronium*, a system made up of an electron and a positron bound together. Models suggest that one fourth of the positronium atoms form in singlet state (or *para-positronium*), characterised by antiparallel electron-positron spins and a mean lifetime of $\tau = 125$ ps. In this configuration, positronium preferentially decays by emitting two 511-keV γ-ray photons (in fact, para-positronium decay can emit any even number of photons, but with lower probability as the number of photons rises). The other positronium atoms settle in a triplet state configuration (or *ortho-positronium*), with parallel spins and a mean lifetime of $\tau = 145$ ns, which preferentially decay producing three γ-ray photons, each with an energy below 511 keV. The prompt γ-ray emission expected for novae is composed of a 511 keV line (fed by direct electron-positron annihilation) and a lower-energy continuum (supplied by positronium decay plus Comptonization of 511-keV photons; see Leising & Clayton (1987); Gómez-Gomar et al. (1998); Hernanz et al. (1999)), with a cut-off at ∼ 20–30 keV due to photoelectric absorption. The existence of such a sharp cut-off precludes the possibility that the hard X-ray flux observed in novae may result from Compton degradation of γ-rays, as indicated in a number of papers (see, e.g., Livio et al. (1992); Suzuki & Shigeyama (2010)). It is worth observing that this is the most powerful γ-ray emission predicted for classical novae (Leising & Clayton 1987; Gómez-Gomar et al. 1998; Hernanz et al. 1999).

Despite the relatively large fluxes expected for this prompt emission, its detection represents a real challenge, as it occurs well before the nova is discovered by optical means. This rules out any chance of repointing a γ-ray satellite once a nova has been singled out. Accordingly, any possibility relies solely on *a posteriori* data analysis, on the track of γ-ray excess release around 511 keV from the direction of novae after their optical observation. To this purpose, data obtained with the TGRS instrument on board the WIND satellite (Harris et al. 1999), with the BATSE instrument on board the Compton Gamma-Ray Observatory (CGRO; Hernanz et al. (2000)), or with the RHESSI satellite (Matthews et al. 2006), has been analysed; however, only upper limits on the ^{18}F annihilation line have been set to date. Current estimates of the maximum detectability distance of the 511 keV line with the SPI spectrometer on board the γ-ray observatory INTEGRAL return a value of ∼ 3 kpc (Hernanz et al. 1999; Hernanz & José 2004). Nonetheless, such evaluations critically depend on an accurate knowledge of the various nuclear processes involved in the destruction and production of ^{18}F during nova outbursts.

Production of ^{18}F in novae is triggered by the ^{16}O(p,γ)^{17}F reaction, which is either followed by ^{17}F(p,γ)^{18}Ne(β^+)^{18}F or by ^{17}F(β^+)^{17}O(p,γ)^{18}F. Owing to the relatively large half-life of ^{18}F ($T_{1/2} = 110$ min), it is mainly burnt by proton-captures, predominantly by ^{18}F(p,α)^{15}O, and to a smaller extent by ^{18}F(p,γ)^{19}Ne (see, e.g., José (2016)). For nova conditions, the most uncertain reaction of the network of nuclear processes cited above is, by far, ^{18}F(p,α)^{15}O. In the last decade this reaction has been extensively studied and, in particular, many investigations have focused on its examination by means of direct measurements at the relevant astrophysical energies. Such

experimental studies are be very challenging not only for the energy range of interest, which leads to vanishingly small cross sections, but also for the reason that ^{18}F is a radioactive isotope, so it requires dedicated facilities to be synthesised. Starting from the beginning of this century many experimental collaborations have attempted to measure the ^{18}F(p,α)^{15}O astrophysical S(E)-factor. A first direct experiment was performed by Bardayan et al. (2002) focusing on the resonance at $E_{c.m.}$=330 keV and its strength. Afterwards, additional experimental investigations were performed by many groups using different experimental approached, see e.g. DeSereville et al. (2009); Beer et al. (2011); Laird et al. (2013). So far, many uncertainties are still present on the low-energy resonances, their widths and interference, thus influencing the evaluation of the reaction rate at the temperatures relevant for astrophysics and, consequently, the nova nucleosynthesis. Therefore new experimental studies, especially centred at the nova Gamow window, are mandatory.

2. THM BASIC FEATURES AND APPLICATION TO THE ^{18}F$(p,\alpha)^{15}$O REACTION

Alternative and valuable approaches to obtain the bare-nucleus cross section (devoid of electron screening effects), σ_b, for charged particles at energies lower than the Coulomb barrier, have been made available by indirect methods. Among them, the Trojan Horse Method (THM) (Spitaleri 1991) is well suited to study binary reactions induced at astrophysical energies by neutrons or charged particles by using convenient reactions with three particles in the exit channel. THM enables us to by-pass both Coulomb barrier suppression and electron screening enhancement, thus making the use of extrapolation unnecessary. In the last two decades, the method has turned out to be very profitable in the application to several aspects of nuclear astrophysics research, such as primordial nucleosynthesis (Pizzone et al. 2014; Tumino et al. 2014), the lithium problem (Pizzone et al. 2005; Lamia et al. 2013), AGB nucleosynthesis (La Cognata et al. 2015; Palmerini et al. 2013), light-element depletion in stars (Lamia et al. 2015). In all these cases, the THM has been applied to the study of reactions between stable nuclei and p, α or, more recently neutrons (Gulino et al. 2013). Therefore, the method can be considered as a rodust indirect technique to deduce bare-nucleus cross section for reactions of astrophysical interest, leading to the establishment of accurate reaction rates.

The basic premises of the THM have been recently reviewed in Tribble et al. (2014); Spitaleri et al. (2016). Here we shall just underscore that it is based on the quasi-free (QF) breakup reaction mechanism, which enable us to indirectly derive the astrophysical factor of a binary process from the measurement of a suitable three-body one. In particular, the QF reaction mechanism specialises in the THM approach, relevant for astrophysical applications. When the energy of the incident particle is chosen large enough to overcome the Coulomb barrier of the interacting nuclei, the breakup of the TH nucleus into a participant and a spectator particle can be regarded as occurring within the nuclear interaction field, so that Coulomb repulsion is greatly suppressed. As a consequence, the THM also becomes insensitive to problems connected with the electron screening, the interaction energies being well above the typical energies at which the atomic degrees of freedom can play a role.

In this paper we will describe a R-matrix analysis of the recent THM measurements of the ^{18}F(p,α)^{15}O cross section, addressing the open questions making the reaction rate more uncertain at the lower temperatures, because of unknown properties of near-threshold resonances and interference between these and higher energies broad states.

The THM was applied to the ^{2}H(^{18}F,α^{15}O)n process to obtain critical information on the ^{18}F(p,α)^{15}O cross section at energies of astrophysical interest, below about 400 keV (Cherubini et al. 2015; Pizzone et al. 2016). In the ^{2}H(^{18}F,α^{15}O)n reaction, the QF break-up was identified and selected, with deuteron splitting into its constituents p and n, whereby n is regarded as the spectator to the ^{18}F(p,α)^{15}O virtual reaction.

According to the Plane Wave Impulse Approximation (PWIA), the differential cross section of the $2 \rightarrow 3$ reaction measured in a α-^{15}O coincidence experiment can be expressed in a form explicitly featuring the one of the binary virtual reaction:

$$\frac{\mathrm{d}^3\sigma}{\mathrm{dE}_\alpha \mathrm{d}\Omega_\alpha \mathrm{d}\Omega_{^{15}\mathrm{O}}} \propto \mathrm{KF}\,|\Phi(\vec{\mathrm{p}}_\mathrm{s})|^2 \left(\frac{\mathrm{d}\sigma}{\mathrm{d}\Omega}\right)^{\mathrm{HOES}} \quad (1)$$

where KF is a kinematical factor, depending on the masses and energies of the detected particles. The experimental spectator momentum distribution $|\Phi(\vec{\mathrm{p}}_\mathrm{s})|^2$ is linked to the $p-n$ relative motion inside deuteron (Lamia et al. 2012b), with $(d\sigma/d\Omega)^{\mathrm{HOES}}$ the half-off-energy-shell (HOES) cross section of the reaction of astrophysical interest (Mukhamedzhanov 2011).

According to the THM premises, the Coulomb barrier is overcome in the entrance channel; thus, the obtained HOES cross section, $(\mathrm{d}\sigma/\mathrm{d}\Omega)^{\mathrm{HOES}}$, is essentially the nuclear part of the ^{18}F(p,α)^{15}O cross section, without the Coulomb barrier suppression and electron screening enhancement. However, the HOES cross section is obtained with an arbitrary normalisation to be matched to the directly measured cross sections, so that direct

data have to be present at energies appropriate for the normalisation procedure. The agreement between the THM and the direct cross sections at high energies and the subsequent scaling represents a necessary validation of the THM, in view of its application to measurements of reactions of astrophysical interest and constitutes a necessary step also for reactions induced by radioactive ion beams, such as the ^{18}F(p,α)^{15}O.

In the last years, an intensive experimental and theoretical activity has been carried out to upgrade the THM approach, with the aim of making normalisation to direct data unnecessary (La Cognata et al. 2009, 2010; Mukhamedzhanov 2011; La Cognata et al. 2013; Trippella & La Cognata 2017). This is an important step in the application of the THM to reactions involving unstable nuclei, since in many cases no direct data exist for normalisation, chiefly in the case of reactions induced by neutrons on unstable nuclei. This novel perspective has also the advantage of fully accounting for HOES effects and of allowing us to extend the THM reach by using more advanced nuclear reaction models, such as the Distorted Wave Born Approximation (DWBA) and the Continuum-Discretised Coupled Channel (CDCC) approaches (La Cognata et al. 2009; Mukhamedzhanov 2011).

Two experimental runs were performed by applying the THM to the ^{2}H(^{18}F,α^{15}O)n reaction and we refer for further details on the experiments and data analysis to Cherubini et al. (2015) for the first run (performed at CNS-RIKEN, hereby RIKEN run) and to Pizzone et al. (2016) for the second run (performed at Texas A&M University, hereby TAMU run). Both data sets are in agreement with each other within the experimental errors and can offer complementary information with respect to the direct measurements. In Fig. 1 the average of the two data sets, weighted over the respective experimental errors, is reported as blue symbols, together with the statistical as well as the normalisation errors. The horizontal error bar marks instead the energy uncertainty, essentially linked to the binning chosen in the data reduction (see Cherubini et al. (2015); Pizzone et al. (2016) for more details).

3. R-MATRIX ANALYSIS OF THE ^{18}F$(p,\alpha)^{15}$O THM S-FACTOR

Guided by the recent work by Bardayan et al. (2015), we have performed a R-matrix analysis of the THM data (Cherubini et al. 2015; Pizzone et al. 2016), with the aim to check the compatibility of the THM S-factor with this recent R-matrix calculation, discussing, updating, combining and analysing the most recent direct and indirect results on the ^{18}F$(p,\alpha)^{15}$O reaction, excluding the THM

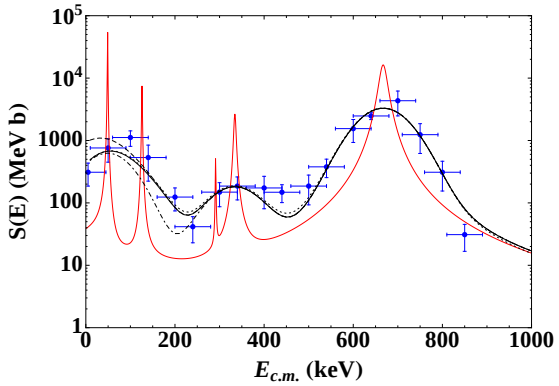

Figure 1. R-matrix analysis of the THM astrophysical factor (blu points), under the assumption of $J^{\pi} = 3/2^{+}$ for the 6460 keV ^{19}Ne state as discussed in Cherubini et al. (2015); Pizzone et al. (2016). The solid black line is the smoothed R-matrix calculation, accounting for a 53 keV energy spread (standard deviation), with parameters given in Tab. 1. The red line is the corresponding deconvoluted astrophysical factor. The dashed black line is the smoothed R-matrix calculation including the 6417 keV level, while the dot-dashed line is the smoothed R-matrix calculation where the 6537 keV is excluded. Finally, the dotted line marks the smoothed R-matrix calculation where the interference signs were changed to (++)(−+).

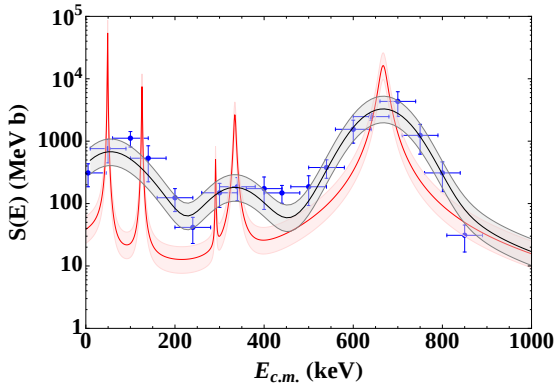

Figure 2. R-matrix analysis of the THM astrophysical factor (blue points) as in Fig. 1. The evaluated uncertainty in the R-matrix fit is reported as a shadowed grey area and as a red band for the corresponding deconvoluted S(E)-factor.

data. The THM S(E) factor is shown as blue symbols in Fig. 1, and is taken from Pizzone et al. (2016) (average of the RIKEN and TAMU run data).

The resonance parameters used in the R-matrix analysis are given in Tab. 1. The same states as in Bardayan et al. (2015) were considered, with the corresponding parameters being taken from Tab. 2. However, to reproduce THM data, some changes have proven necessary, following the discussion in Cherubini et al. (2015); Pizzone et al. (2016). In detail, the best fit curve (shown as a solid black line in Fig. 1) is achieved by assum-

Table 1. Parameters of the R-matrix calculation (red line) in Fig. 1. Resonance energies, corresponding levels in ^{19}Ne, spin-parities, Γ_p and Γ_α are reported, respectively. The 7 keV state is also shown, even though it is not needed to reproduce the THM data.

E_{res} (keV)	E_x (keV)	J^π	Γ_p (keV)	Γ_α (keV)
-124	6286	$1/2^+$	83.5[a]	11.6
7	6417	$3/2^-$	$1.6\,10^{-41}$	0.5
29	6440	$1/2^-$	$3.8\,10^{-19}$	220
49	6460	$3/2^+$	$2.3\,10^{-13}$	0.9
126	6537	$7/2^+$	$7.1\,10^{-8}$	1.5
291	6702	$5/2^+$	$2.4\,10^{-5}$	1.2
334	6745	$3/2^-$	$2.2\,10^{-3}$	5.2
665	7075	$3/2^+$	15.2	23.8
1461	7872	$1/2^+$	55	347

[a]Since this is a sub threshold resonance, the ANC in $fm^{1/2}$ is cited.

ing the (++)(++) interference pattern, according to the notation in Fig. 3 of Bardayan et al. (2015), excluding the 7 keV resonance, attributable to the occurrence of a $3/2^-$ state of ^{19}Ne at 6417 keV energy, and introducing a $7/2^+$ state of ^{19}Ne at 6537 keV, as remarked in Cherubini et al. (2015); Pizzone et al. (2016). The (++)(++) notation is used to point our that the relative interference signs between the -124 and 1461 keV resonances is (++) (first pair) and the ones of the 47 and 665 keV resonances is (++) as well (second pair). The corresponding astrophysical factor, given by the red line in Fig. 1, has been smeared to account for the experimental energy resolution, which has been evaluated in Cherubini et al. (2015) and equals 53 keV (standard deviation), leading to the solid black line. For 18 degrees of freedom, a reduced $\chi^2 = 1.5$ is obtained in this case.

Alternative solutions were checked, to see if they cannot be excluded based on THM data. First, we have performed the same calculation including the 6417 keV state. After smoothing, the dashed black line in Fig. 1 is obtained, resulting in a reduced $\chi^2 = 3.1$ for 18 degrees of freedom. The incompatibility of the THM experimental S-factor with the calculation including the 7 keV resonance can be quantitatively estimated if the deviation with respect to the assessed uncertainty is calculated at 5 keV, the experimental point closer to the resonance centroid. A simple algebra leads to a disagreement at the 5.5σ level, making us confident that in this case the adjustment of the parameters in Bardayan et al. (2015) is well reasonable. However, since our result is based on a single experimental point, more work is mandatory to rule out a contribution from this level. This resonance causes an increase of the smoothed astrophysical factor below 100 keV (see Fig. 1), which is incompatible with THM results, the reduced χ^2 being a factor of two larger in this last case. Such result is consistent with the absense of observation of the mirror state in the reanalysis of the ^{15}N$(\alpha,\alpha)^{15}$N cross section (Bardayan et al. 2005).

Focusing on the 126 keV resonance, which is mentioned by Cherubini et al. (2015); Pizzone et al. (2016) but not included in the R-matrix calculation by Bardayan et al. (2015), the corresponding smeared S-factor is shown as a dot-dashed black line in Fig. 1. In this case, a reduced $\chi^2 = 1.8$ is deduced, larger than the best fit case (namely, 1.5) but probably not enough different to definitely claim its occurrence. Finally, the sensitivity of the THM S-factor on the interference pattern has been tested, by switching from the (++)(++) relative signs to the (++)(−+) combination, that is, assuming constructive interference between the $3/2^+$ states. We focus on these patterns as they involve states observed in the THM measurements (Cherubini et al. 2015; Pizzone et al. 2016). After including energy resolution effects, the dotted curve in Fig. 1 is retrieved, almost undistinguishable from the best fit curve (solid black line). Therefore, the energy resolution affecting the present THM S-factor is not enough to pick the most likely interference pattern, energy resolution washing out eventual differences. Similar results are obtained if the (−+)(++) and (−+)(−+) combinations are used, because of the poor energy resolution affecting the THM experimental points. Other interference schemes were not taken into account since they are presently excluded (see discussion in Bardayan et al. (2015)). This result supports further THM measurements of the ^{18}F$(p,\alpha)^{15}$O THM S-factor, which might prove very useful to single out the most likely interference pattern since it makes it possible to reach the energies of astrophysical interest, at odds with present-day direct measurements. It is also worth noting that, because of the energy resolution, the weak 6440 and 6702 keV states were not reported in Cherubini et al. (2015); Pizzone et al. (2016). Energy smearing, in fact, almost completely suppresses their contribution in comparison with the one of the neighbour more intense resonances. Therefore, future THM measurements need to aim at improved energy resolution, even if the quality of radioactive ion beams today available set a limit at the resolution which can be achieved.

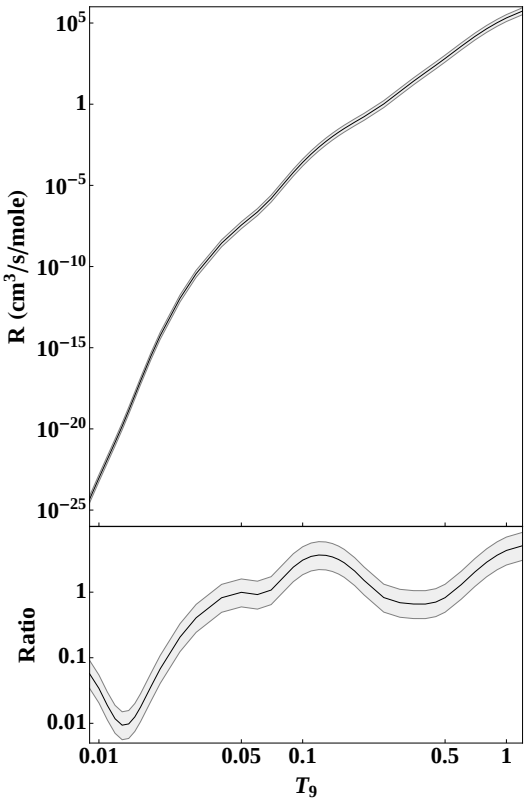

Figure 3. Upper panel: $^{18}F(p,\alpha)^{15}O$ reaction rate calculated using the deconvoluted THM S-factor (red line of Fig. 1). Lower panel: ratio of the THM reaction rate to the one reported in the JINA REACLIB database (Cyburt et al. 2010). In both plots the uncertainties of the reaction rate are represented as a a shadowed band.

Table 2. Reaction rate as a function of the temperature.

T_9	R_{ij} [cm^3 mol^{-1} s^{-1}]
0.007	2.49673×10^{-28}
0.008	1.47096×10^{-26}
0.009	4.68148×10^{-25}
0.01	9.39356×10^{-24}
0.015	1.15888×10^{-18}
0.02	5.63177×10^{-15}
0.03	3.6577×10^{-11}
0.05	3.57743×10^{-8}
0.1	0.000260867
0.15	0.0187306
0.2	0.168753
0.25	1.03239
0.3	5.96964
0.35	26.049
0.4	87.1969
0.45	249.303
0.5	654.916
0.6	3668.36
0.7	14842.5
0.8	44314.9
0.9	104398
1	206150

For the best fit curve we have performed an error estimate, by fitting the upper and lower limits set by the uncertainties affecting the experimental data. The resulting error bands affecting the R-matrix calculations are reported in Fig. 2 as a shadowed grey band and as a red band for the smoothed and the deconvoluted S(E)-factor, respectively.

4. CALCULATION OF THE REACTION RATE

The reaction rate of the THM deconvoluted astrophysical factor, given by the red line of Fig. 1, has been calculated using standard equations (Iliadis 2007). The resulting reaction rate is shown in the upper panel of Fig. 3 as a function of the temperature, expressed in units of 10^9 K ($T_9 = T/10^9$ K), and listed in Tab. 2. For comparison, in the lower panel of the same figure, the ratio of the THM reaction rate to the one reported in the JINA REACLIB database (Cyburt et al. 2010) is also displayed. The latter is the interpolation of the Iliadis et al. (2010) reaction rate using a standard formula (Cyburt et al. 2010), differing at most by 10% from the original calculation. We are juxtaposing the THM rate with the Cyburt et al. (2010) one since the latter is commonly used in novae modelling. In the temperature region of interest for astrophysics, $0.1 \lesssim T_9 \lesssim 0.5$, an increase in the reaction rate ratio is observed, compatible with the results by Bardayan et al. (2015). The absence of the 7 keV resonance, whose occurrence is not supported by THM data, determines a decrease of the reaction rate ratio below such temperature, even if the astrophysical consequences of this modification are likely to be negligible. The uncertainties arising from the present measurement are fully accounted for and reported in Fig. 3 as a shadowed band.

The extracted reaction rate has significant astrophysical implications especially in the novae temperature range, where a larger rate with respect to Cyburt et al. (2010); Bardayan et al. (2002) is calculated.

5. ASTROPHYSICAL IMPLICATIONS

To examine the impact of the new determination of the ^{18}F(p,α)^{15}O rate on nova nucleosynthesis, a series of one-dimensional, hydrodynamic simulations have been performed with the SHIVA code (José & Hernanz 1998; José 2016). Two models of 1.25 $M_\odot$ oxygen-neon white dwarfs, accreting H-rich material from the stellar companion at a rate of 2×10^{-10} $M_\odot$ yr^{-1}, have been computed with identical input physics except for the prescription adopted for the ^{18}F(p,α)^{15}O rate (Models D and D'). While no change on the dynamical properties of the explosion is found (e.g., peak temperature attained, amount of mass ejected), Tab. 3 reveals important differences in the chemical composition of the ejected matter, with a net reduction in the mean ^{18}F content by a factor $^{18}F_{D'}/^{18}F_D \sim 2.1$, which reduces previous estimates of the detectability distance of the 511 keV annihilation line by γ-ray satellites by a factor $\sim \sqrt{2}$. Note, as well, that larger amounts of ^{18}O and a net reduction of ^{19}F by a $\sim 20\%$ are also found when the new ^{18}F(p,α)^{15}O rate, rather than the prescription reported in Iliadis et al. (2010), is used.

Four additional models (Models A, B, C and E), covering a wide range of masses for the accreting white dwarf (i.e., two carbon-oxygen white dwarfs of 1 $M_\odot$ and 1.15 $M_\odot$, and two oxygen-neon white dwarfs of 1.15 $M_\odot$, and 1.35 $M_\odot$), have also been computed. Results are summarised as well in Tab. 3. All these models result in a net reduction of the final ^{18}F content when compared with models computed with the Iliadis et al. (2010) rate.

6. CONCLUDING REMARKS

In this work we have assessed the impact of the recent indirect measurement of the ^{18}F(p,α)^{15}O cross section by means of the THM (Cherubini et al. 2015; Pizzone et al. 2016) on the synthesis of carbon, nitrogen, oxygen and fluorine isotopes in novae, as well as the changes of the dynamics of the explosion. This has been achieved inserting the calculated reaction rate into the SHIVA code (José & Hernanz 1998; José 2016) and comparing the output with the results obtained by considering the ^{18}F(p,α)^{15}O reaction rate of Iliadis et al. (2010).

To calculate the reaction rate, the THM data in Cherubini et al. (2015); Pizzone et al. (2016) could not be used as they are because of the energy resolution affecting the indirect astrophysical factor. Therefore, based on the recent work of by Bardayan et al. (2015), we have performed a R-matrix analysis of the THM S(E) to deduce the infinite resolution astrophysical factor. In this way we have been able to supply a reaction rate devoid of experimental effects, which can be juxtaposed to other results in the literature, consistently propagating the uncertainties on energy and on S(E). From this analysis, it turns out that THM data tend to disfavour the contribution of the 6417 keV state of ^{19}Ne, while supports the occurrence of the 126 keV resonance in the ^{18}F(p,α)^{15}O astrophysical factor.

As a consequence of the THM S(E), the reaction rate shows an increase right at novae temperatures (peak values of $T_9 \sim 0.1 - 0.5$). While the explosion dynamics is not affected, the chemical composition of the ejected material shows significant differences when the THM reaction rate is used. In particular, the ^{18}F content in the nova ejecta reported in this work demonstrates a factor of about 2 decrease, reducing the detectability distance by a factor of about 1.4.

Software: SHIVA (José & Hernanz 1998; José 2016)

REFERENCES

Bardayan, D.W., Batchelder, J. C., Blackmon, J. C., et al. 2002, Phys. Rev. Lett. 89, 262501

Bardayan, D.W., Kozub, R.L., & Smith, M.S. 2005, Phys. Rev. C 71, 018801.

Bardayan, D.W., Chipps, K.A., Ahn, S., et al. 2015, Phys. Lett. B, 751, 311

Beer, C.E., Laird, A. M., Murphy, A. St. J., et al. 2011, Phys. Rev. C, 83, 042801(R)

Cherubini, S., Gulino, M., Spitaleri, C., et al. 2015, Phys. Rev. C, 92, 015805

Clayton, D.D. 1981, Astrophys. J., 244, L97

Clayton, D.D. & Hoyle, F. 1974, Astrophys. J., 187, L101

Coc A. , Hernanz, M., Jose, J., & Thibaud, J.P. 2000, Astron. Astrophys., 357, 561

Cyburt, R.H., Amthor, A.M., Ferguson, R., et al. 2010, Astrophys. J. Suppl. Ser., 189, 240

De Sereville, N., Angulo, C., A. Coc, A., et al. 2009, Phys. Rev. C, 79, 015801

Diehl, R. 2010, AIP Conference Proceedings, 1269, 144

Gómez-Gomar, Hernanz, José, J., & Isern, J., 1998, Mon. Not. Roy. Astron. Soc., 296, 913

Gulino, M., Spitaleri C., Tang X., et al. 2013, Phys. Rev. C, 87, 12801

Harris, M. J., Naya, J. E., Teegarden, B. J., et al. 1999, Astrophys. J., 522, 424

Table 3. Mass-averaged composition in the nova ejecta (CNOF-group elements).

	Model A	Model B	Model C	Model D	Model D'	Model E
WD	CO	CO	ONe	ONe	ONe	ONe
M_{wd} ($M_\odot$)	1	1.15	1.15	1.25	1.25	1.35
Reference	This Work	This Work	This Work	This Work	Iliadis et al. (2010)	This Work
^{12}C	4.52E-2	4.76E-2	2.28E-2	2.61E-2	2.61E-2	2.21E-2
^{13}C	1.10E-1	7.87E-2	2.15E-2	2.54E-2	2.55E-2	1.56E-2
^{14}N	1.18E-1	1.33E-1	3.36E-2	4.15E-2	4.15E-2	5.47E-2
^{15}N	9.63E-3	3.66E-2	3.57E-2	5.66E-2	5.66E-2	1.07E-1
^{16}O	2.40E-1	2.23E-1	1.09E-1	6.12E-2	6.11E-2	5.97E-3
^{17}O	4.74E-3	1.15E-2	2.90E-2	3.67E-2	3.68E-2	4.05E-2
^{18}O[a]	3.09E-7	5.67E-7	1.49E-6	2.09E-6	4.59E-6	8.81E-6
^{18}F[a]	7.14E-7	1.29E-6	3.48E-6	4.82E-6	1.03E-5	1.98E-5
^{19}F	2.03E-8	1.86E-8	3.62E-8	1.19E-7	1.40E-7	1.42E-6

[a]Values correspond to 1 hr after peak temperature was achieved in the envelope.

Hernanz, M., José, J., Coc, A., et al. 1999, Astrophys. J., 526, L97

Hernanz, M., Smith, D.M., Fishman, J., et al. 2000, AIP Conference Proceedings, 510, 82

Hernanz, M. & José, J. 2004, 5th INTEGRAL Workshop "the INTEGRAL Universe" (ESA SP-552). Ed. V. Schnfelder, G. Lichti & C. Winkler, p.95

Hernanz, M. 2008, Classical Novae, 2nd Edition (Cambridge: Cambridge Astrophysics Series), p. 252

Hernanz, M. 2014, Stella Novae: Past and Future Decades (San Francisco: Astronomical Society of the Pacific Conference Series), p. 252

Iliadis, C. 2007, Nuclear Physics of Stars (New York: Wiley)

Iliadis, C., Longland, R., Champagne, A.E., et al. 2010, Nucl. Phys. A, 841, 31

José, J, & Hernanz, M., 1998, Astrophys. J., 494, 680

José, J, & Hernanz, M., 2007, J. Phys. G: Nucl. Part. Phys., 34, R431

José, J., & Shore, S. N. 2008, Classical Novae, 2nd Edition (Cambridge: Cambridge Astrophysics Series), p. 121

José, J. 2016, Stellar Explosions: Hydrodynamics and Nucleosynthesis (Boca Raton: CRC/Taylor and Francis)

La Cognata, M., Goldberg, V., Mukhamezhanov, A.M., et al. 2009, Phys. Rev. C, 80, 012801

La Cognata, M., Spitaleri C., Mukhamezhanov A., et al, 2010, Astrophys. J., 723, 1512

La Cognata, M., Spitaleri C., Trippella O., et al, 2013, Astrophys. J., 777, 143

La Cognata, M., Palmerini, S., Spitaleri, C., et al. 2015, Astrophys. J., 805, 128

Laird, A., Parikh, A., Murphy, A. St. J. et al. 2013, Phys. Rev. Lett., 110, 032502

Lamia, L., Spitaleri, C., La Cognata, M., et al. 2012, Astron. Astrophys., 541, 158

Lamia, L., La Cognata, M., Spitaleri, C., et al. 2012, Phys. Rev. C, 85, 025805

Lamia, L., Spitaleri, C., Pizzone, R.G., et al. 2013, Astrophys. J., 768, 65

Lamia, L., Spitaleri, C., Tognelli, E., et al. 2015, Astrophys. J., 811, 99

Leising, M. D., & Clayton, D. D. 1987, Astrophys. J., 323, 159

Livio, M., Mastichiadis, A., Oegelman, H., et al. 1992, Astrophys. J., 394, 217

Matthews, T. G., Smith, D. M. & Hernanz, M. 2006, 38, 344

Mukhamedzhanov, A. 2011, Phys. Rev. C, 84, 044616

Palmerini, S., Sergi, S., La Cognata, M., et al. 2013, Astrophys. J., 764, 128

Pizzone, R.G., Tumino A., Degl'Innoccenti, S., et al. 2005, Astron. Astrophys., 438, 779

Pizzone, R.G., Spartá, R., Bertulani C., et al. 2014, Astrophys. J., 786, 112

Pizzone, R.G., Roeder B., McCleskey, M., et al. 2016, Eur. Phys. J. A, 52, 24

Spitaleri C. 1991, in Problems of Fundamental Modern Physics II, Ed. by R. Cherubini, P. Dalpiaz, and B. Minetti (Singapore: World Scientific), p. 21

Spitaleri, C., Lamia, L., Puglia, S.M.R., et al. 2014, Phys. Rev. C, 90, 035801

Spitaleri, C., La Cognata, M., Lamia, L., et al. 2016, Eur. Phys. J. A, 52, 77

Starrfield, S., Iliadis, C., & Hix, W.R. 2008, Classical Novae, 2nd Edition (Cambridge: Cambridge Astrophysics Series), p. 77

Starrfield, S., Iliadis, C., & Hix, W.R. 2016, Publ. Astron. Soc. Pac., 128, 051001

Suzuki, A., & Shigeyama, T. 2010, Astrophys. J. Lett., 723, L84

Tribble, R.E., Bertulani, C., La Cognata, M., et al. 2014, Rep. Prog. Phys., 77,106901

Tumino, A., Spartá, R., Spitaleri, C., et al. 2014, Astrophys. J., 785, 96

Trippella, O., & La Cognata, M. 2017, Astrophys. J., 837, 41